

SINTEZA ȘI CARACTERIZAREA UNOR ELECTROLIȚI SOLIZI PE BAZĂ DE CeO₂ PENTRU CELULE DE COMBUSTIE DE TEMPERATURĂ INTERMEDIARĂ

SYNTHESIS AND CHARACTERIZATION OF SOLID ELECTROLYTES BASED ON CeO₂ FOR INTERMEDIATE TEMPERATURE FUEL CELLS

GEORGETA VELCIU^{1,2}, ALINA MELINESCU^{2*}, VIRGIL MARINESCU¹, VICTOR FRUTH³,
RAREȘ SCURTU³, MARIA PREDĂ²

¹ Institutul Național de Cercetare-Dezvoltare pentru Inginerie Electrică ICPE-CA Splaiul Unirii nr.313, sector 3, București, 030138

² Universitatea POLITEHNICA București - Facultatea de Chimie Aplicată și Știința Materialelor, Splaiul
Independenței nr. 313, 060042

³ Institutul de Chimie-Fizică „Ilie Murgulescu” al Academiei Române, Splaiul Independenței nr. 202, 060021,
București, România

Four compositions in the range of 85-90 % CeO₂, the other being SrO, CaO or Y₂O₃ combined two or three were studied. The mixtures have been homogenized by a wet route for 10 hours. After drying the obtained powders were subjected to thermal analysis which showed that in the process of grinding chemical changes occur. The apparent and relative densities were measured on the samples sintered at temperatures of 1350 and 1400°C resulting that the relative densities of the samples are between 79 and 92%. X-ray diffraction revealed that the main mineralogical compound of the samples, thermally treated in the range of 1300-1400°C, is a solid solution with a structure of fluorite type specific to CeO₂. For some samples were also identified CaY₄O₇ and SrCeO₃, compounds resulting by solid-phase reactions and two solid solutions of the type SrCe_{0,85}Y_{0,15}O_{2,95} and (Ce,Y)₂O₃. The microstructure of the studied samples was investigated by electron microscopy and the results showed that the samples exhibit rounded and needle-shaped grains of different sizes. Electrical measurements have shown that three of samples have a corresponding behavior to solid electrolytes usable for IT-SOFC cells.

S-au studiat patru compoziții în care CeO₂ variază de la 85-90%, restul fiind SrO, CaO sau Y₂O₃ combinați câte doi sau trei. Amestecurile au fost omogenizate în mediu umed timp de 10 ore. După uscare pulberile obținute au fost supuse analizelor termice care au arătat că, în procesul de măcinare, apar modificări chimice. Pe probele sinterizate la temperaturile de 1350 și 1400°C s-au determinat densitățile aparente și relative acestea din urmă, pentru cele patru probe, fiind cuprinse între 79 și 92%. Componentul mineralogic principal prezent în probele tratate termic în intervalul 1300-1400°C, determinat prin difracție de raze X, este o soluție solidă cu structură de tipul fluorină specifică CeO₂. În unele probe s-au mai identificat SrCeO₃ și CaY₄O₇ compuși rezultați prin reacții în fază solidă și două soluții solide de tipul SrCe_{0,85}Y_{0,15}O_{2,95} și (Ce,Y)₂O₃.

Textura probelor a fost studiată prin microscopie electronică, probele fiind caracterizate prin granule rotunjite de diferite dimensiuni sau aciculare. Măsurătorile electrice efectuate au arătat că trei dintre probe au o comportare corespunzătoare electrolitelor solizi utilizabili pentru celulele SOFC-IT.

Keywords: solid electrolytes, LSGM, microwave technique, IT-SOFC.

1. Introduction

SOFC type fuel cells have been widely studied [1] and normally operate at temperatures above 1000°C, in which case are used electrolytes based on solid solutions of zirconium oxide [2]. It is very important to increase efficiency and to expand their use at portable instruments, by decreasing of temperature operating in the range 400-700°C. For this purpose can be used ceramics of CeO₂ that is in present intensively studied. From these ceramics can obtain solid electrolytes, which can be used for fuel cells with an intermediate temperature of operation, which directly converts the energy of a fuel into electricity and heat. This is due to the fact that they have an ionic conductivity at temperatures

of 700-800°C, greater than the stabilized zirconium oxide. Also, in this temperature range CeO₂ is thermodynamically stable under variable conditions of the environment. In order to increase the ionic conductivity, in composition of the electrolytes based on CeO₂ are introduced the cations with a lower valence than tetravalent cerium. In this way in the network of fluorite type occur anionic vacancies, which increase the mobility of the oxygen ions. There are numerous studies that show that in this effect can be used divalent (Ca²⁺, Sr²⁺) [3] or trivalent (Gd³⁺, Sm³⁺, Y³⁺) cations [3-7]. It has been shown that by using some of them greatly decreases conductivity at the boundary between grains due to lack of anionic vacancies, so in the present paper are studied the materials with

* Autor corespondent/Corresponding author,
E-mail: alina.melinescu@gmail.com

ternary composition [8-9] when are used simultaneously two cationic substituent's.

Another important issue by obtaining of electrolytes based of CeO₂ is weak tendency at sintering, sintering temperature of pure ceria being over 1500^oC, and at these temperatures occur problems related to its reduction by loss of oxygen. For improvement of the sintering process besides cationic oxides which creates vacancies it can introduce oxides which improve sintering especially MnO₂ [10-13].

In this paper, were studied synthesis and electrical properties of some samples with CeO₂ – main component and beside of this has been used other two or three oxides soluble in its fluorine type network.

2. Experimental

The chemical composition of the synthesized samples is presented in Table 1.

Table 1

The oxide compositions of the samples sintered (% mass)
Compoziția oxidică a probelor sintetizate (% masice)

Sample no. Nr. probă	CaO	SrO	Y ₂ O ₃	CeO ₂
E1	5	5	-	90
E2	5	-	5	90
E3	-	5	5	90
E4	5	5	5	85

The first three samples are placed in ternary systems because contain beside cerium dioxide other two oxides. The fourth sample contains CeO₂ and other three oxides, what makes to possess a quaternary composition. The samples were synthesized by solid phase reactions using as starting materials CaCO₃, SrCO₃, Y₂O₃ and CeO₂ chemical purity (Fluka). The samples were mechanically homogenized by wet route in the mill with zirconia balls, the ratio of balls:solid material being 1:1 and the grinding time being 10 h. The obtained mixtures were dried in an oven at 120^oC to constant weight. They were uniaxially pressed at 100 MPa into tablets with a diameter of 20 mm and a height of 5 mm. The pressed samples were thermally treated at 1300-1400^oC with a plateau at the maximum temperature for two hours. Apparent density of the obtained samples was measured by Archimedes method. Relative density was calculated by reporting at density of the cerium oxide. The mineralogical phases formed during the thermal treatment were identified by X-ray diffraction, in the 2θ from 20^o to 70^o, using CuKα radiation with the Shimadzu 6100 diffractometer. The microstructure of the samples was examined by electron microscopy with FESEM-FIB apparatus, Auriga Workstation. The measurements of impedance spectroscopy, in air in the temperature range 200 to 800 ^oC were made on the samples synthesized and thermally treated at 1400^oC. The real and the imaginary part of the complex impedance were recorded in the frequency range of 1Hz-1MHz with frequency

analyzer Solartron SI 1260. Spectra were recorded in the temperature ranges equal to 50 degrees Celsius.

3. Experimental results

3.1. Thermal behavior

The thermal behavior was studied by differential thermal analysis on the resulting powders after drying with a thermal analysis apparatus Jupiter STA 449 F3. Thermal analysis curves for the sample E1 are shown in Figure 1.

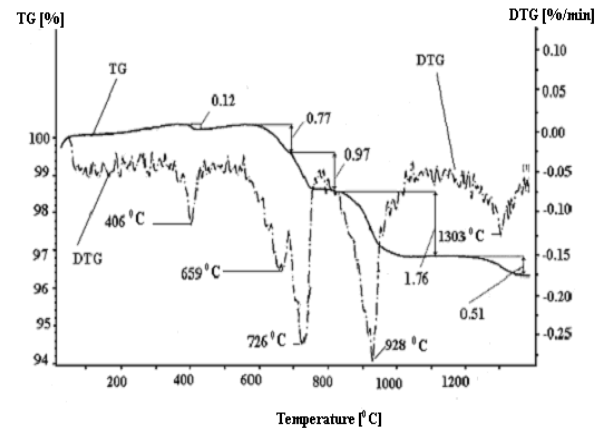


Fig. 1 - Thermal analysis curves for the E1 sample / Curbele de analiză termică pentru proba E1.

Thus on DTG curve is observed the presence a five effects accompanied by weight loss. The first of these is at 406^oC and can be assigned to removal of water from Ca (OH)₂, which results from partially dissociation of the calcium carbonate in the process of grinding. The effect from temperature of 726^oC can be assigned to dissociation of calcium carbonate. The dissociation of calcium carbonate takes place normally at a temperature of 930^oC, the effect being shifted to lower temperatures due to the fact that the grinding decreases the degree of crystallinity of the raw materials. Similar changes occur at strontium carbonate in the sense that it is partially transformed in Sr(OH)₂, which dissociates in this case at 659^oC. Strontium carbonate dissociates at 928^oC, which is also a lower value compared to 1100-1150^oC which is normal temperature of dissociation. It results that due to long time of milling in the raw materials arise some modifications. On the diagram shown appears at 1303^oC, a mass loss of 0.51%, which can be assigned to elimination of a part of oxygen from network of CeO₂ which is affected at a rate of 10.96%. As shown in Table 1, ceria is found in excess and remains in a high proportion in the free state. The weight variation occurs because of variable valence of cerium, which passes from valence state Ce⁴⁺ to Ce³⁺. This phenomenon does not result in a change of the network but only leads to the formation of oxygen vacancies in network of fluorite type of the cerium oxide [14].

Figure 2 shows the thermal analysis curves for sample E2, consisting of calcium carbonate, yttrium oxide and cerium oxide.

There is on DTG curve three effects, the first at 956°C corresponds to the elimination of carbon dioxide from calcium carbonate. In this case, the dissociation temperature is higher than the pure calcium carbonate, probably due to the diffusion of the yttrium ions into the grains of calcium carbonate. Between yttrium oxide and cerium oxide is formed two solid solutions namely, cerium oxide is soluble in yttrium trioxide and vice versa [15,16], and in both cases there is a partial reduction of cerium oxide as it evidenced by

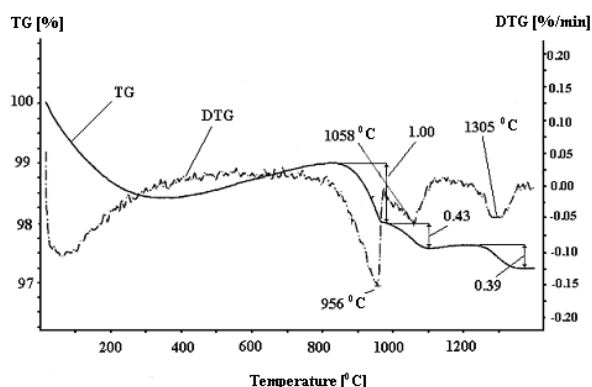


Fig. 2 - Thermal analysis curves for the E2 sample / Curbele de analiză termică pentru proba E2.

effects of loss of mass at temperatures 1058 and 1305°C. Taking into account the losses recorded at thermal treatment results that at the first effect turns a proportion of 9.24% CeO₂, and at the second 8.39%.

Thermal analysis curves for the sample E3 are shown in Figure 3, where one can observe the presence of four effects accompanied by weight loss. As in the case of sample E1, it is found that the presence of strontium carbonate which, mechanic turns leads to the appearance of Sr(OH)₂ which lose the water to 645°C and at 724°C takes place removal the carbon dioxide from the strontium carbonate. The basic environment created it made as a part of Y₂O₃ to transform in

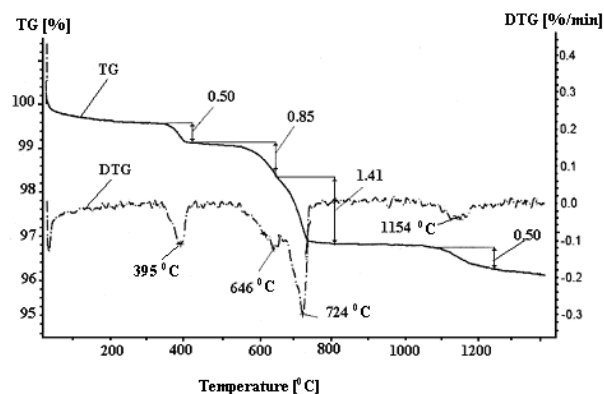


Fig. 3 - Thermal analysis curves for the E3 sample / Curbele de analiză termică pentru proba E3.

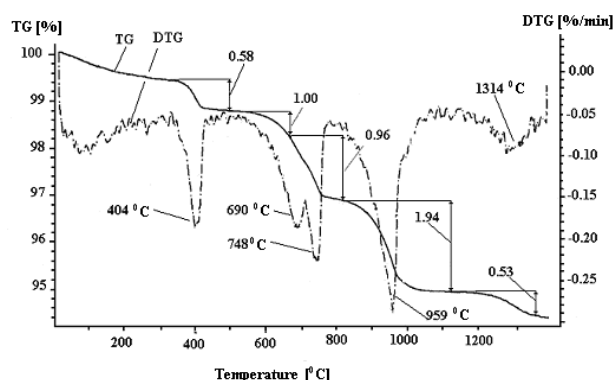


Fig. 4 - Thermal analysis curves for the E4 sample / Curbele de analiză termică pentru proba E4.

the Y(OH)₃, which dissociates to 395°C. Effect from 1154°C, is accompanied by mass loss due to the elimination of oxygen from network of cerium oxide. The fourth sample with the most complex chemical composition (Figure 4) has five effects on the DTG curve.

The first effect, which is under full speed at 404°C, represents the cumulative effect of the loss of mass from hydroxides of calcium and yttrium.

The second effect from 690°C shows removal of water from strontium hydroxide, and the decomposition of calcium carbonate appears at 748°C. Carbon dioxide from SrCO₃ is removed at a temperature of 959°C. In this case, it is found at 1340°C an effect with a loss of oxygen in network of CeO₂ and a proportion of oxide of 11.39% is affected.

Table 2

The density of sintered samples depending on the temperature of heat treatment
Densitatea probelor arse în funcție de temperatura de tratament termic

Sample no. Nr. probă	Temperature, °C Temperatură	Apparent density, g/cm ³ Densitate aparentă	Relative density, % Densitate relativă
E1	1350	5.73	82
	1400	6.26	89
E2	1350	5.54	79
	1400	5.90	84
E3	1350	6.46	92
	1400	6.34	90
E4	1350	5.51	79
	1400	6.04	86

The obtained samples by pressure were thermally-treated at temperatures of 1350 and 1400°C, for two hours at the maximum temperature and on these were measured the apparent and relative density. The obtained results are shown in Table 2 and it is found a variation in relative density between 79 and 92%.

The E3 sample shows a good tendency at sintering, after a thermally treated at temperature of 1350°C having a relative density over 90%. The E2 and E4 samples however, show a lower tendency to sintering, which at 1400°C have the relative densities of only 84% and 86% respectively.

3.2. Mineralogical composition

The mineralogical composition of the four samples was determined by X-ray diffraction and the obtained patterns were plotted as a function of the temperature of the thermal treatment. Figure 5 presents the diffraction patterns for E1 sample thermally treated at 1300, 1350 and 1400°C. It is noted that regardless of thermal treatment temperature occur only specific diffraction lines of cerium oxide.

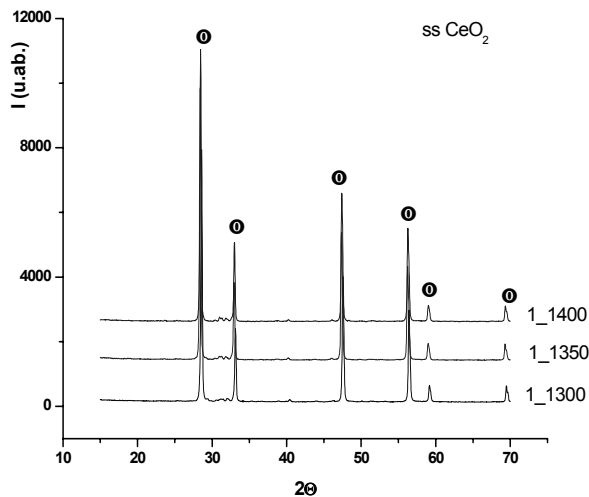


Fig. 5 - X-ray diffractogram of the E1 sample X-ray diffraction spectra of the sample E1 depending on the temperature of thermal treatment / *Spectrele de difracție de raze X pentru proba E1 în funcție de temperatura de tratament termic.*

This fact shows that the two oxides of calcium and strontium were solubilised in network of cerium oxide to form a solid solution. In the case of E2 sample the X-ray diffraction pattern is presented in Figure 6, where it is also apparent that the two oxides CaO and Y_2O_3 formed a solid solution with cerium oxide. Although by thermal analysis were found losses of mass resulting from the elimination of the partial oxygen from CeO_2 network, these take place with the formation of oxygen ions vacancies, and cerium trioxide was not revealed in the X-ray patterns, but by electron microscopy could identify the type of solid solution $(\text{Ce},\text{Y})_2\text{O}_3$.

In Figure 7 the X-ray pattern of the E3

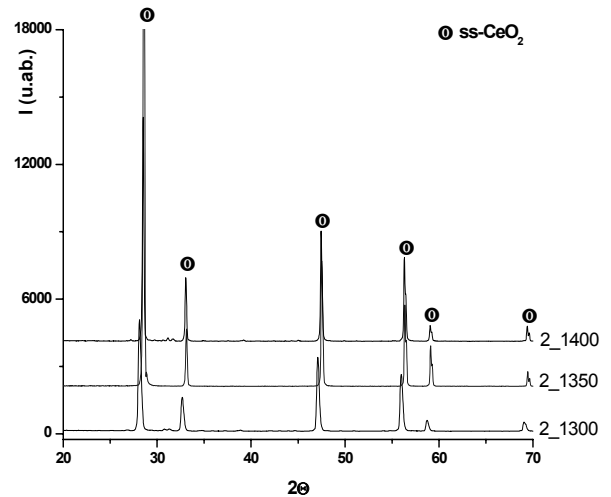


Fig. 6 - X-ray diffractogram of the E2 sample X-ray diffraction spectra of the sample E2 depending on the temperature of thermal treatment / *Spectrele de difracție de raze X pentru proba E2 în funcție de temperatura de tratament termic.*

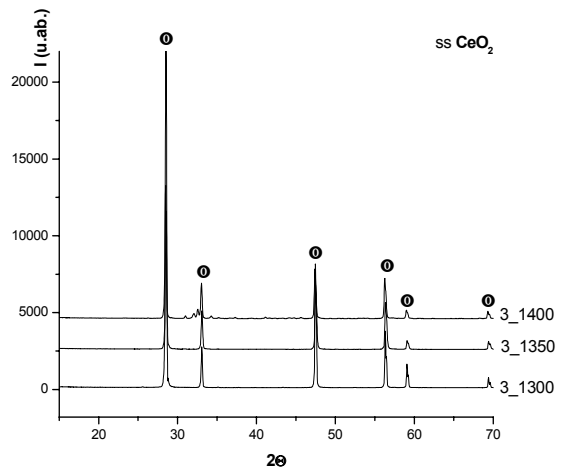
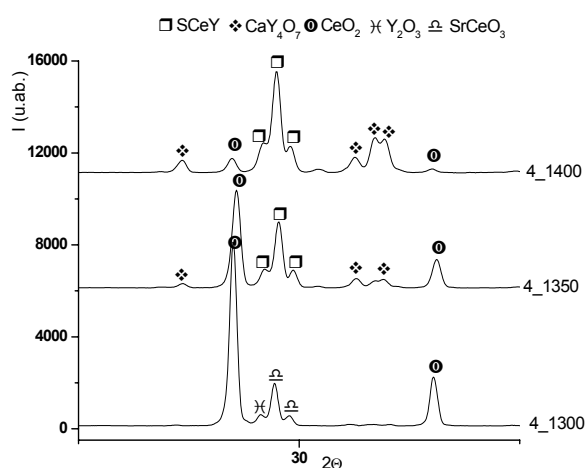


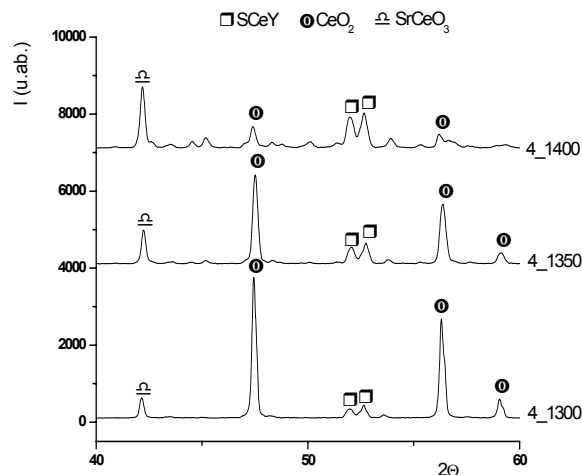
Fig. 7 - X-ray diffractogram of the E3 sample X-ray diffraction spectra of the sample E3 depending on the temperature of thermal treatment / *Spectrele de difracție de raze X pentru proba E3 în funcție de temperatura de tratament termic.*

sample is presented. The E3 sample displays only one type of crystalline phase namely CeO_2 . This can be a consequence of solubilization of the two oxides, of strontium and yttrium in its network.

Referring the sample E4, which has a most complex composition, being formed of four oxides of cerium, calcium, strontium and yttrium, the solid phase reactions that occur are more complicated. Thus at temperature of 1300°C (Figure 8 a, b) were identified beside cerium and yttrium oxides, a binary compound SrCeO_3 and a solid solution $\text{SrCe}_{0,85}\text{Y}_{0,15}\text{O}_{2,95}$ formed by partial solubilization of yttrium oxide in SrCeO_3 . At temperature of 1350°C yttrium oxide does not appear in the pattern because reacted with CaO and formed CaY_4O_7 . At temperature of 1400°C the mineralogical composition of the sample consists from two compounds SrCeO_3 and



a



b

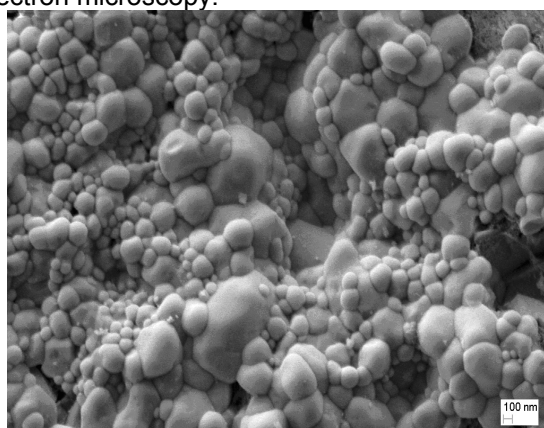
Fig.8 - X-ray diffractogram of the E4 sample X-ray diffraction spectra of the sample E4 depending on the temperature of thermal treatment / Spectrele de difracție de raze X pentru proba E4 în funcție de temperatura de ardere.

CaY₄O₇ and two solid solutions, the first with a fluorite type structure of CeO₂ and the second with an orthorhombic type structure SrCe_{0,85}Y_{0,15}O_{2,95}.

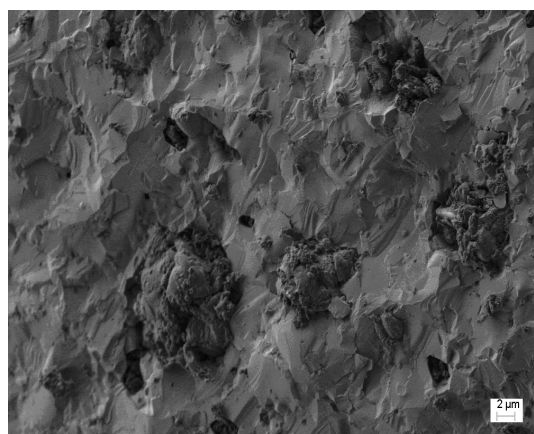
3.3. Microstructure

The microstructure of the studied samples was examined for all samples with the scanning electron microscopy.

Thus, from Figure 9 that corresponding to sample E1 at nanometer scale there is a relatively homogenous microstructure. However at micron scale (Figure 9b), one can observe the presence of the agglomerates corresponding binary compound SrCeO₃ formation. This being in low proportion could not be identified by X-ray diffraction.

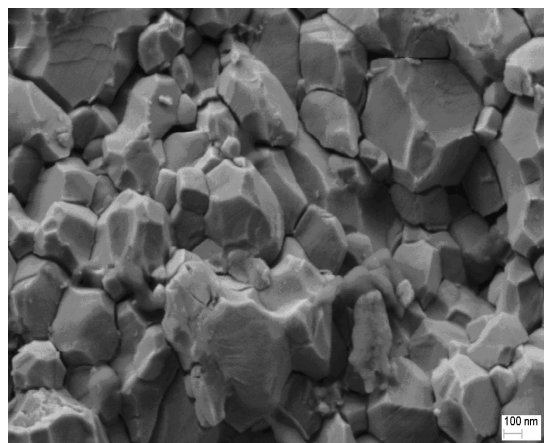


a)

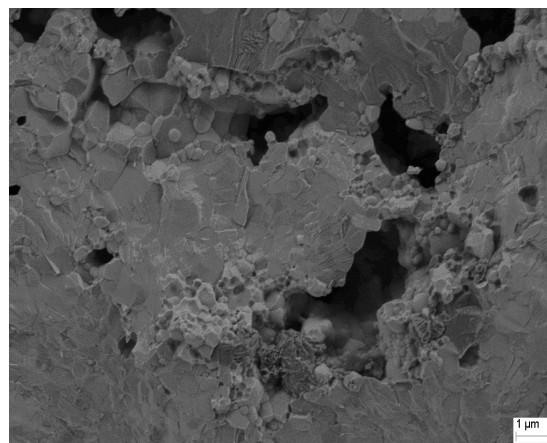


b)

Fig. 9 (a,b) - Scanning electron microscopy images of the E1 sample / Imaginile electronmicroscopice pentru proba E1.



a)



b)

Fig. 10 (a,b) - Scanning electron microscopy images of the E2 sample / Imaginile electronmicroscopice pentru proba E2.

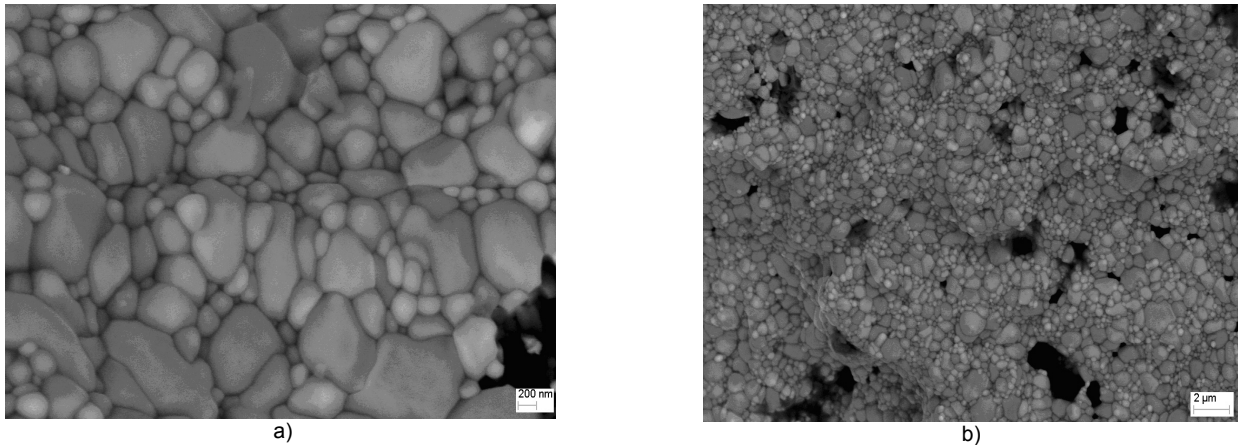


Fig. 11 (a,b) - Scanning electron microscopy images of the E3 sample / *Imaginile electronmicroscopice pentru proba E3.*

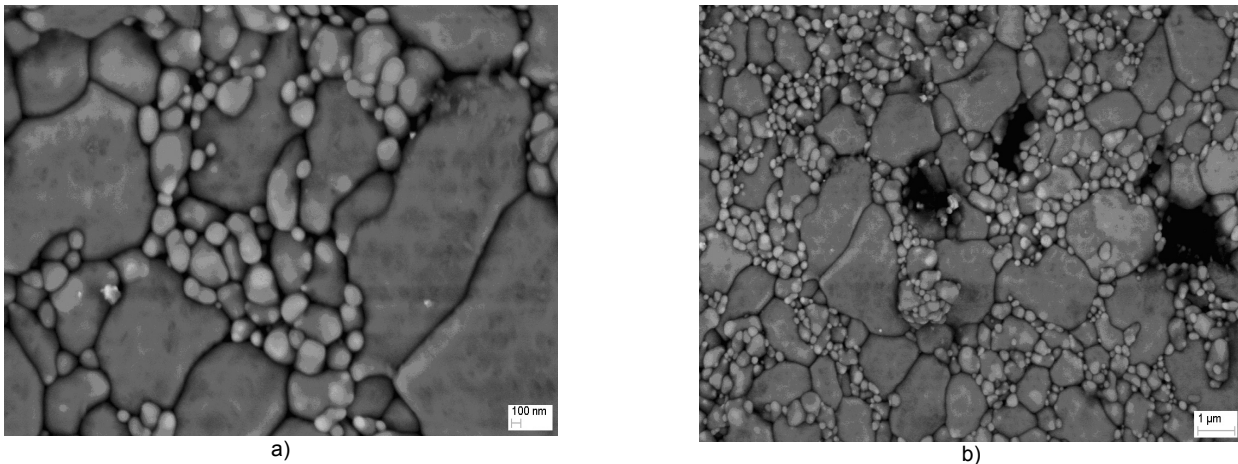


Fig. 12 (a,b) - Scanning electron microscopy images of the E4 sample / *Imaginile electronmicroscopice pentru proba E4.*

Scanning electron microscopy image of the sample E2 at high magnification shows also a uniform microstructure (Figure 10a), but are seen in Figure 10b, the presence of the solid solution of the type $(\text{Y,Ce})_2\text{O}_3$ in the form of needle-like granules.

Regarding E3 sample Figure 11(a,b) was observed a much homogeneous microstructure compared to other samples.

For the sample 4 Figure 12(a,b) presented large differences in terms of grain size. Small granules are located at the boundary between large grains and constituting a intergranular space.

3.4. Electrical properties

Solid electrolytes ionic conductors, are characterized by the impedance spectra are generally divided into three areas, which show the contribution at resistance of the granules, resistance at grains boundaries and the resistance at interface electrode/electrolyte at total resistance of the system [17,18].

The impedance spectra for the sample E1 are shown in Figure 13(a,b) corresponding to temperatures of 500 to 750K.

In Figure 13 one can clearly see the two semicircles corresponding contribution of the two

types of resistance, i.e. inside of granules and at limits between granules. The two semicircles show almost equal participation of both types of resistance to the total resistance. The third semicircle is attributed to polarization at limit electrolyte/electrode and its existence implies that in this case conductivity is mainly ionic. At temperature of 750 K the deformation is more pronounced for both semicircles. This can be explained by the chemical in homogeneity at the boundary between grains and the vacancies mobility change with temperature [18-20]. Also, it can take into account a partial diffusion of the two into cerium oxide, and their segregation at the almost equal participation of both types of resistance to the total resistance. The third oxides boundary between grains [21-23]. Impedance spectrum for the E2 sample is shown in Figure 14, where it is found only one semicircle.

This can be explained by the presence of a type of the solid solution $(\text{Y,Ce})_2\text{O}_3$ located in particular at the boundary between grains. The impedance spectra of sample E3, are shown in Figure 15 where is distinguished at 500 and 650K the presence of three distinctive regions which indicate the influence on total conductivity, of the conduction inside grains and between grains,

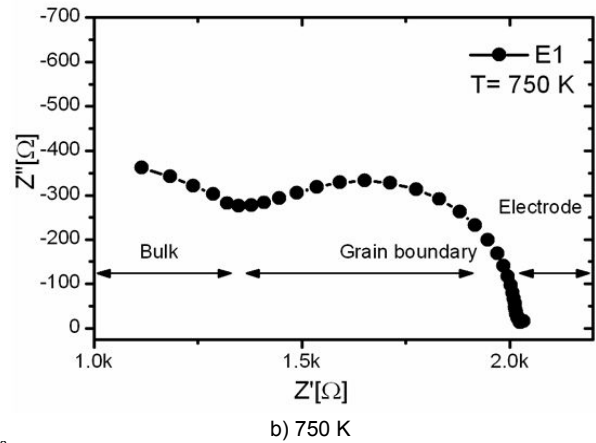
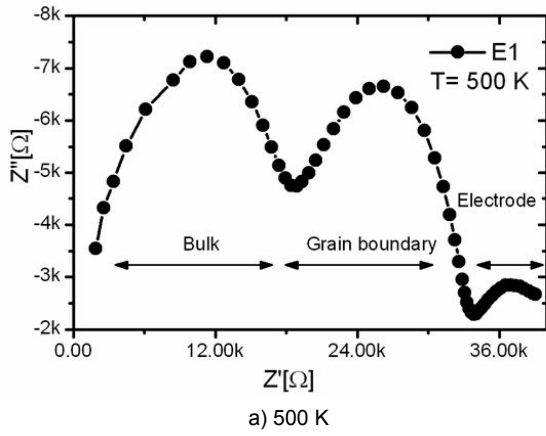


Fig. 13 - E1 impedance spectra for the sample heat treated at 1400°C / Spectrele de impedanță pentru proba E1 tratată termic la 1400°C.

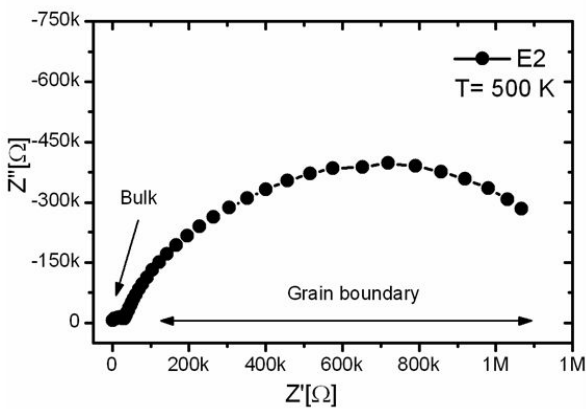


Fig. 14 - Impedance spectra for the E2 sample at 500K / Spectrul de impedanță pentru proba E2 la temperatura de 500K.

which can be seen and for E4 sample (Figure 16).

The contribution of the grain boundary to total resistance can be determined by factor of blocking f_R , which is calculated according to the formula:

$$f_R = \frac{R_{gb}}{R_b + R_{gb}}$$

where R_b is the resistance in the grains and R_{gb} resistance at boundary of grains. This factor represents the ratio between the number of charge carriers trapped at the interface under the experimental conditions applied and the total number of charge carriers in the sample [24]. The obtained results are given in Table 3.

Table 3

The variation of the blocking factor
Variația factorului de blocare

Sample Proba	Temperature, Temperatura [K]	Blocking factor Factor de blocare
E1	500	0,47
	750	0,65
E3	500	0,78
	650	0,70
E4	500	0,37
	700	0,43

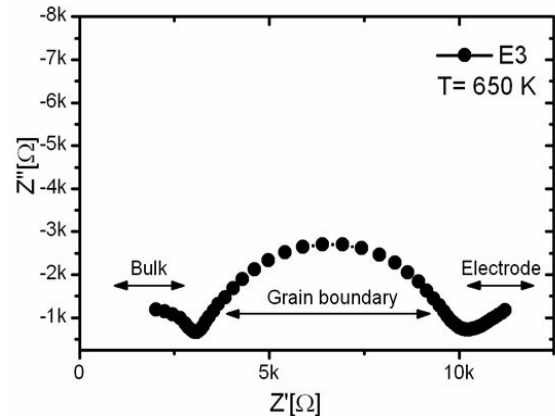
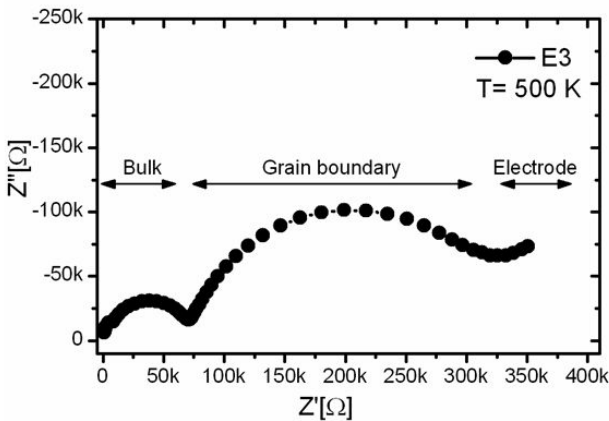


Fig.15 - Impedance spectra for the E3 sample / Spectrele de impedanță pentru proba E3.

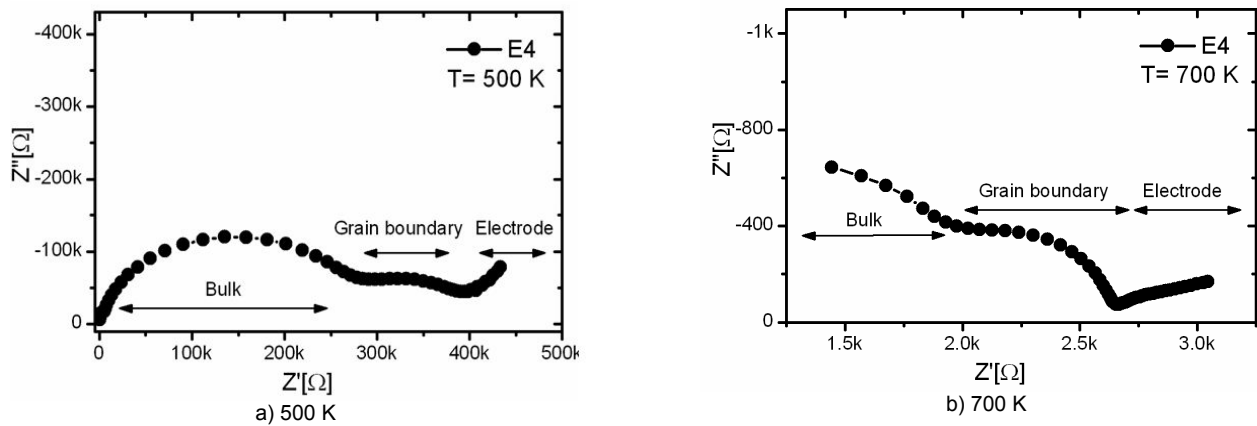
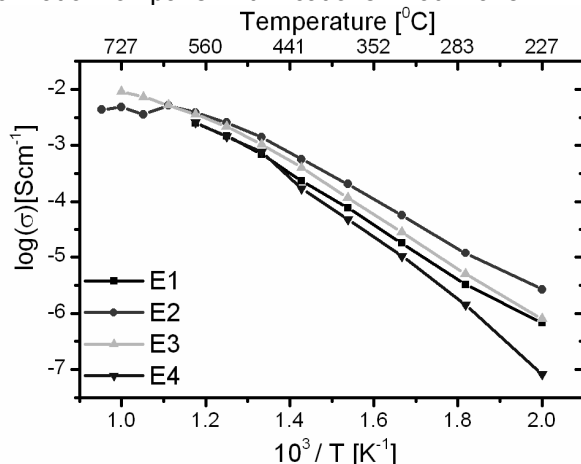


Fig. 16 - Impedance spectra for the E4 sample / Spectrele de impedanță pentru proba E4.

It is noted for the sample E1, at a temperature of 500K a blocking factor equal to 0.47, showing that the involvement of the two components to the total resistance, i.e. resistance into grains and intergranular resistance is almost equal. At temperature of 750K the factor of blocking increases, what shows that predominant becomes intergranular space. For the E3 sample predominantly is resistance of intergranular space and corresponding blocking factor shows a slight decrease as a function of temperature. Regarding E4 sample is observed that prevailing grains resistance and factor of blocking increases with rising temperature of measurement.

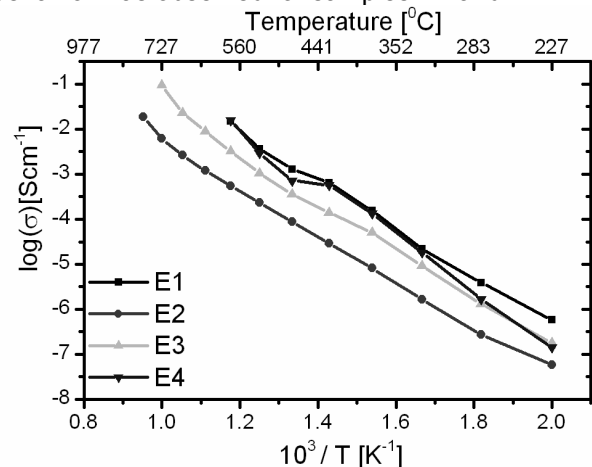
The different aspect of the impedance spectra may be explained by the influence of the point defects in solid solution grains which are first the type of solubilized ions in network of cerium oxide. They can create tensions in network due to their size and distribution. Secondly the difference of valence between the tetravalent ion of cerium and the cations solubilized (divalent or trivalent) which lead to apparition of the oxygen vacancies which allow to oxygen to move more easily in the network, but that can also contribute to the formation of pairs with cations what make

Fig. 17 - The variations of the electrical conductivity intragranular (σ_G) dependence of temperature / Variația conductivității electrice intragranulare (σ_G) în funcție de temperatură.

perturbations occur. Characteristic spectrum of intergranular area is influenced by the presence of some phases on surface of the granules which may be oxides or chemical compounds formed by solid state reactions that have different conductivity compared to granules. In addition the behavior of specimens may also depend on the temperature at which the determination has been made. Such variations can be attributed and microstructure observing that, for small grains predominate intergranular conduction and for large granules the conductivity in inside of the granules [20,24].

In Figures 17-19 are represented the variations of the electrical conductivity dependence of temperature for granules, the intergranular space and the total conductivity of the four samples sintered.

Thus, in Figure 17 can be observed greater differences of conductivity in grains at low temperature. At temperatures higher than 500⁰K, the electrical conductivity of the four samples is nearly identical. Figure 18 presents the variation of the conductivity of the samples at the boundary between the granules and an almost identical behavior was observed for samples E1 and E4

Fig. 18 - The variations of the electrical conductivity intergranular (σ_{GB}) dependence of temperature / Variația conductivității electrice intergranulare în funcție de temperatură.

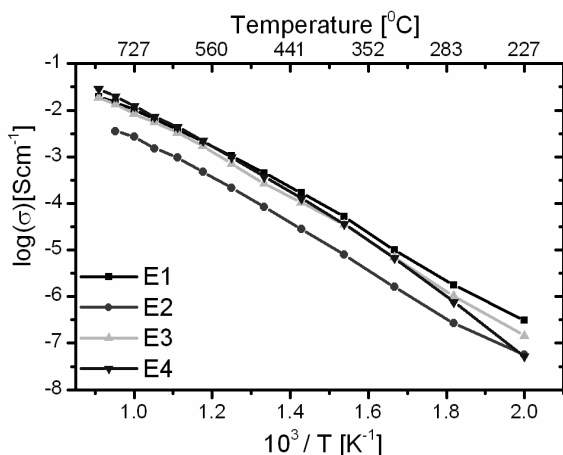


Fig. 19 - The variations of the electrical conductivity total dependence of temperature / Variația conductivității electrice totale în funcție de temperatură.

throughout the temperature range studied. The conductivity difference is quite small between the two samples mentioned and E3 sample. A greater difference is found with the sample E2, for which at elevated temperature can be higher with one order of magnitude.

Variation of the total conductivity of the four samples is given in Figure 19, where is noticed a similar behavior for the samples E1, E3 and E4. In general, the behaviour of the samples is linear, suitable for operation at fuel cells with intermediate temperature and have conductivity needed to operate into fuel cell at a temperature between 600 and 750°C.

4. Conclusions

Four samples with a composition based on CeO₂ and CaO, SrO and Y₂O₃ oxides were studied. Because of the long time of milling, some raw materials have undergone chemical changes which were revealed by thermal analysis. Strontium carbonate partially dissociates thus creating a powerful basic environment, which induces some transformations of CaCO₃ and Y₂O₃. For all the studied samples a partial dissociation of CeO₂ was also observed. It should be noted that it does not exist diffraction lines corresponding to Ce₂O₃ identified by X-ray diffraction. This fact shows that the losses of mass observed are accompanied by formation of vacancies of the oxygen in the network of cerium oxide. The thermal treatment in the studied temperature range showed that all the samples have the relative density of between 79 and 92%. X-ray diffraction study has shown that the main phase that forms especially in ternary compositions is a solid solution with a structure of fluorite type specific to CeO₂. The quaternary composition contains beside of two solid solutions also other phases such as compounds formed by chemical reactions in the solid phase. The microstructure of the samples, determined by scanning electron microscopy,


revealed the presence of rounded granules of various sizes. The measurements of impedance have shown that the main mechanism of conduction is the ionic and three of the four samples have corresponding behavior of solid electrolytes. Blocking factors, calculated have showed that at increasing of measurement temperature may increase or decrease, modifying being influenced of intergranular layer. Change in electrical conductivity depending on the temperature of the two components, the intragranular and intergranular is linear and the total conductivity of the samples is corresponding to their use as solid electrolytes for fuel cells of the type of IT-SOFC.

REFERENCES

- Hiroshi Kawamoto, Research and Development Trends in Solid Oxide Fuel Cell Materials, QUARTELY REVIV 6/January 2008, **2**, 52.
- Boudghene Stambouli, and E. Traversa, Solid oxide fuel cells (SOFCs): a review of an environmentally clean and efficient source of energy, Renewable and Sustainable Energy Reviews 2002, **6**, 433.
- F.Zhang, S.W.Chan, J.E.Spanier, E.Apak, Q. Jin, R.D. Robinson and J.P. Herman, Cerium oxide nanoparticles: Size selective formation and structure analysis, Applied Physics Letters, 2002, **80** (1), 127.
- O.P.Shing, T.I.Ping and T.Y.Y. Hin, Mechanochemical Synthesis and characterization of Calcium-doped Ceria Oxide Ion Conductor, IOP Conf. Series: Materials Science and Engineering 2011, **17**, 1.
- M.Yan, T.Mori, J.Zou and J. Drennan, Effect of Grain Growth on Densification and conductivity of Ca-Doped CeO₂ Electrolyte, J.Am.Ceram.Soc. 2009, **92** (11), 2745.
- S.K. Tadokoro, T.C. Porfirio, R. Muccillo, and E.N.S. Muccillo, Synthesis, sintering and impedance spectroscopy of 8 mol% yttria-doped ceria solid electrolyte, Journal of Power Sources 2004, **130**, 15.
- M. Dudek and J. Molenda, Ceria-yttria-based solid electrolytes for intermediate temperature solid oxide fuel cell, Materials Science-Poland, 2006, **24** (1), 45.
- M.Tavafoghi Jahromi and M.J.Tan, Effects of sintering on Y₂O₃-doped CeO₂, Journal of Achievements Materials and Manufacturing Engineering, 2009, **34** (2), 130.
- Doo Kang Kim, Pyeong-Seok Cho, Jong-Heun Lee, Doh-Yeon Kim, Hyun-Min Park, Graeme Auchterlonie, and John Drennan, Mitigation of Highly Resistive Grain-Boundary Phase in Gadolinia-Doped Ceria by the Addition of SrO, Electrochemical and Solid-State Letters, 2007, **10**, 5 B91.
- L. Xiao, K. Sun and X. Xu, Catalytic combustion of methane over CeO₂-MO_x(M=La³⁺, Ca²⁺) solid solution promoted Pd/γ-Al₂O₃ catalysts, Acta Phys.-Chim.Sin., 2008, **24** (11), 2108.
- M. Preda, and A. Melinescu, Cerium oxide sintering using strontium oxide as additive, Romanian Journal of Materials, 2009, **39** (1), 50.
- Tianshu Zhang, Peter Hing, Haitao Huang, and J. Kilner, Sintering study on commercial CeO₂ powder with small amount of MnO₂ doping, Materials Letters **57**, 2002, 507.
- Chunwen Sun, Hong Li and Liquan Chen, Nanostructured ceria-based materials: synthesis, properties, and applications, Energy Environ. Sci., 2012, **5**, 8475
- P.O. Maksimchuk, A.A. Masalov, and Yu.V. Malyukin, Spectroscopically Detected Formation of Oxygen Vacancies in Nano-Crystalline CeO₂ - x, Journal of Nano- and Electronic Physics, 2013, **5** (1), 4

15. L. Li , O. Van Der Biest, L. Wang , J. Vleugels , W.W. Chen, and S.G. Huang, Estimation of the phase diagram for the ZrO₂-Y₂O₃-CeO₂ system, *Journal of the European Ceramic Society* **21**, 2000, 2903.
16. V.Longo, and L.Podda, Phase equilibrium diagram of the system ceria-yttria for the temperatures between 900 and 1700°C, *J.Mater.Sci.*, 1981, **16** (3), 839.
17. Derek C Sinclair, Characterization of Electro-materials using ac Impedance Spectroscopy, *Bol. Soc. Esp. Cerám. Vidrio*, 1995, **34** (2), 55.
18. P. Jasinski, V. Petrovsky, T. Suzuki, and H. U. Anderson, Impedance Studies of Diffusion Phenomena and Ionic and Electronic Conductivity of Cerium Oxide, *Journal of The Electrochemical Society*, 2005, **152** (4), J27.
19. Henry L. Tuller, Ionic conduction in nanocrystalline materials, *Solid State Ionics* 2001, **31**, 143.
20. E.N.S. Muccillo , D.M. Avila, Impedance spectroscopy of tetragonal zirconia polycrystals doped with ceria, *Materials Letters*, 2002, **56**, 454.
21. P.S.Cho, S.Y. Park, J.J. Kim, H.S.Do, H.M.Park and J.H.Lee, Diffusion induced grain-boundary migration in SrO-doped CeO₂ electrolyte and its effect on electrical properties, *Solid State Ionics*, 2010, **181**, 1420.
22. Eliana N. S. Muccillo and M. Kleitz, Ionic Conductivity of Fully Stabilized ZrO : MgO and Blocking Effects, *Journal of the European Ceramic Society* 1995, **15**, 51.
23. Zhenwei Wang, Mojie Cheng, Zhonghe Bi, Yonglai Dong, Huamin Zhang, Jing Zhang, Zhaochi Feng, Can Li, Structure and impedance of ZrO₂ doped with Sc₂O₃ and CeO₂, *Materials Letters*, 2005, **59**, 2579.
24. K. Obal, Z. Pedzich, T. Brylewski, and M. Rekas, Modification of Yttria-doped Tetragonal Zirconia Polycrystal Ceramics, *Int. J. Electrochem. Sci.*, 2012, **7**, 6831.

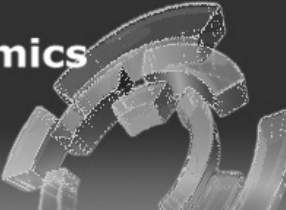
MANIFESTĂRI ȘTIINȚIFICE / SCIENTIFIC EVENTS



5th International Congress on Ceramics

Aug. 17th-21st, 2014

Beijing International Convention Center, Beijing, China



5th International Congress on Ceramics (ICC5) 2014 August 17-21, 2014, Beijing, China

The **5th International Congress on Ceramics (ICC5) 2014** will be held in Beijing, China on August 17-21, 2014.

The **5th International Congress on Ceramics (ICC5) 2014** is a conference and exhibition organized by ceramic societies around the world and is dedicated to the future of the ceramics & glass industry and technology in areas such as Biology and Medicine, Aerospace, Environment, Energy and Transportation, Electro-, Magnetic-, Optical-Ceramics and Devices, Nanostructured Ceramics, Infrastructure, Workforce Development, Security and Strategic Materials.

The **5th International Congress on Ceramics (ICC5) 2014** includes an exhibition showcasing the latest commercially available materials, equipment, products, and services for ceramics and glass.

The **International Congress on Ceramics (ICC)** brings together Ceramic and glass marketing managers, Ceramic and glass business leaders, Product planners and managers, Scientists and engineers from industry, government, and academia, students and R&D managers.

Contact: <http://www.icc-5.com/index.html>
